Linking molecular and continuum mechanics with application to biomimetic nanomaterials and brittle fracture

Bernd Markert, Sandeep P. Patil
markert@iam.rwth-aachen.de

Abstract

The mechanical properties of hierarchically structured materials relies on the characterization and understanding of their nanostructure. A classical example is the dragline silk. Experimental studies have shown that the extraordinary mechanical properties of silk are conferred largely to the nanostructure. In the first part, we propose a three dimensional (3D) finite element model of a silk fiber, which is based on the secondary (nano-scale) structure of the *Araneus diadematus* silk fiber, taking into account the plasticity of the β-sheet crystals as well as the viscous behavior of the amorphous matrix. Our bottom-up approach to dragline silk fiber predicted mechanical properties agree with the experimental ones within the limits of the experimental accuracy. In the second part, a novel combined method for highly brittle materials such as aragonite crystals is proposed, which provides an efficient and accurate in-sight understanding for multi-scale fracture modeling. In particular, physically-motivated molecular dynamics (MD) simulations are performed for crack modeling on the nano-scale, whereas a macroscopic modeling of fracture has proven successful using the diffusive phase-field modeling (PFM) approach. A link between the two modeling schemes is proposed by deriving PFM parameters from the MD atomistic simulations. Thus, in this combined approach, MD simulations provide a more realistic meaning and physical estimation of the PFM parameters.
The proposed computational approach, not requiring any empirical parameters, contributes towards an improved understanding of mechanics at all length-scale levels. Hence, it is an efficient model for the design of new materials as well as applicable to other semi-crystalline polymeric systems or composite materials.

1 Introduction

Molecular dynamics simulations are an efficient approach to study objects on the nanometer scale. They become impracticable when the investigated system has significantly larger dimensions, i. e., on the meso or macroscale. Large-scale simulations of protein materials are not feasible using MD simulations, neither macroscale

structural and mechanical properties can be straightforwardly inferred from MD simulations due to the complexity of biological systems. Typical MD simulations can nowadays be performed on systems containing hundred thousands, or, perhaps, millions of atoms, and for simulation times ranging from a few hundred nanoseconds to more than one millisecond. These numbers are certainly respectable but one may run into conditions where time and/or size limitations become important. On the other hand, continuum structural mechanics can significantly extend the length and time scale of the system.

Continuum structural mechanics is a classical method applicable at all scales. Here, as its name suggests, atomic details of the object are disregarded to focus on the effect of the discretized structure on mechanics. In certain cases, such as determining an elastic modulus of a rubber band, or understanding the stress bearing pattern of a building, the atomic details are normally not the determinant of the property under investigation. In such cases, the object or parts thereof are treated as a continuum sharing the same physical properties. This approach has invincible computational efficiency by greatly reducing the complexity, but is only applicable as long as the continuum approximation is adequate. The hierarchical nanoscale structure of silk renders FEM unfeasible on the small scale, since the atomostic structure crucially defines the material's mechanics. Figure 1 shows a hierarchical structure of spider dragline silk. Crystalline units, the amorphous phase (representative unit) and a combination of both are studied using MD simulations. However, molecular simulations of additional crystalline units and the amorphous matrix are computationally unfeasible. In conjunction to MD, FEM allows to carry out simulations of individual constituents, combinations of them, and full fiber of dragline silk, provided the appropriate parameters, obtained for instance by MD simulations.

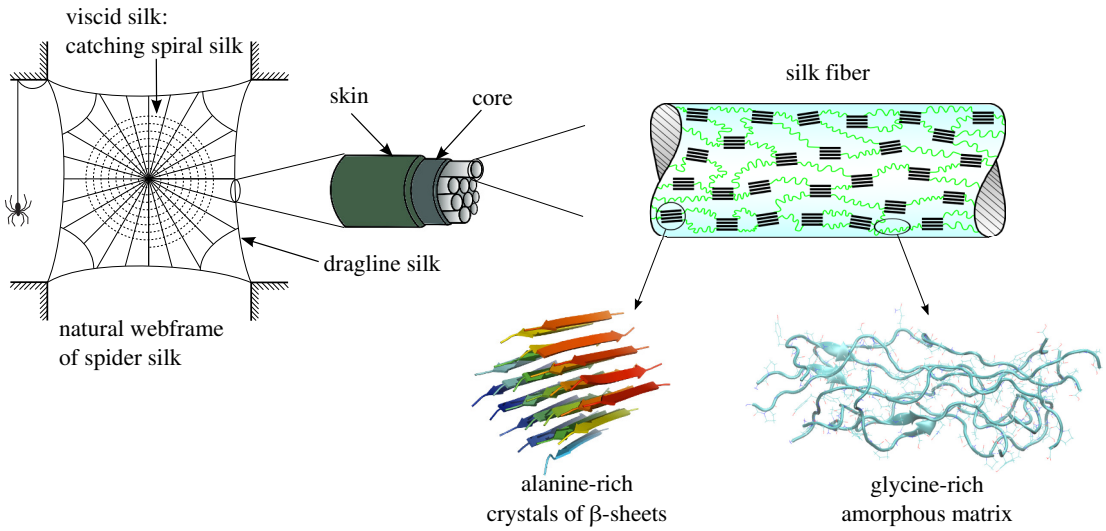

Figure 1: Schematic representation of the spider dragline silk fiber architecture, highlighting the more viscous catching spiral silk (dotted black line), and the much tougher web-frame and dragline silk. Dragline silk fibers are mainly composed of alanine-rich stiff nano-crystals of β-sheets in the glycine-rich disordered peptide chains, whose composition is shown schematically. Figure adopted from [37].

Using different levels of simplifications, continuum mechanics is able to tackle problems for structure sizes that cannot be reached by MD simulations. In spite of the conceptual differences between continuum mechanics and all-atom simulations, the combination of these two different methods is promising. Parameters for continuum mechanics can be obtained from all-atom simulations to ensure high accuracy. The efficiency of continuum mechanics allows to infer mechanical properties on the macroscopic scale from the molecular scale, which is the key to understand a material's interplay of the atomic structure and its overall performance. Here, continuum mechanics and all-atom MD simulations are employed for the silk fiber modeling.
Thus, a bottom-up computational approach is used in this work with the aim to create a bridge between molecular level properties and macroscopic mechanical behavior. In this approach, first, all atom simulations are carried out to obtain key mechanical properties and structural parameters, which are then used to develop a macroscopic model using FEM. In this work, this approach is discussed with the brittle fracture of aragonite crystals.

2 Brittle Fracture of Aragonite Crystals

Molecular Dynamics (MD) simulations are considered new computational methods that are employed to describe the time evolution of a system of interacting particles. They require the numerical solution of Newton's equations for every particle governed by an interatomic potential, i. e., bonded and non-bonded potentials, keeping track of the evolution of the system in space. Due to their real time scales (pico seconds), MD methods are perfectly suited to study the high-speed crack propagation of brittle materials, as demonstrated in the work of Rountree et al. [30]. Additionally, there have also been some applications of the method for a variety of inorganic crystals, such as Si_3N_4 [16], SiO_2 [31], 3C-SiC [17], and GaAs [34]. Although these studies have provided valuable in-sights into crack dynamics, a systematic analysis of mechanical properties at an atomistic scale, as well as a link to the macroscopic continuum mechanical approaches are still not well established.
Nowadays, typical MD simulations can be performed on systems containing hundreds of thousands, or perhaps, a few millions of atoms for simulation times ranging from a few hundred nanoseconds up to a millisecond. These numbers are certainly respectable, but one may run into conditions, where size and/or time limitations become important. The challenges related to the limited dimensions or time scales can be tackled by upscaling MD parameters and frameworks through continuum models. In fact, as it has been shown in numerous other studies, i. e., [5, 26, 27, 28], the mechanical behavior of a given continuous material can be reproduced in a different scale by using mechanical parameters derived directly from atomistic MD simulations.
In what numerical modeling regards, phase-field modeling (PFM) has emerged as a powerful tool to model brittle fracture under a macroscopic continuum approach, offering a good accordance between numerical treatment, accuracy, and computational costs. The pioneering works related to an elastic energy-based approach to describe brittle fracture, namely the works of Griffith [9] and Irwin [15], as well as the variational formulations presented in [4, 8], can be considered as the pillars of

a well-established energy-based framework for brittle fracture. In the past decades, many PFMs, which approximate the sharp edges of the crack by a diffusive interface, have been developed. Due to their simple implementation, these models are able to predict quasi-static and dynamic cases of brittle and ductile fracture, considering diferent fracture modes and loadings, under several discretization schemes [4, 8, 3, 11, 22, 35, 19, 21].
Consequently, this research work pursues to establish a link between the understanding of brittle fracture of a material at an atomistic scale and its macroscopic mechanical features. To this end, an aragonite ($CaCO_3$) tablet undergoing fracture is studied, using both MD and PFM. Herein, the key mechanical properties (e. g., Young's modulus, Poisson's ratio), as well as the phase-field transition width (ϵ) and the mechanical energy release rate (G) of an aragonite crystal are obtained *ab initio*. These physical properties are subsequently employed to reproduce a nanoscale model under a continuous PFM approach.
Given that PFM and MD are relatively new topics in the realm of mechanics, the second and third sections of this work will briefly introduce the implementation of both methods. In the fourth section, a thorough description and brief evaluation of the numerical experiments in MD, as well as PFM are presented. The last section is dedicated to the conclusion and outlook of the present work.

2.1 Materials and MD Simulations

In the present work, MD and PFM simulations are employed to describe the behavior under fracture of Aragonite ($CaCO_3$), a highly brittle ceramic and major constituent of nacre (95 % vol.). Tablets of this material were modeled, as seen in Fig. 2, by using the software Visual Molecular Dynamics (VMD) [14]. One double-notched tablet model was built with length (l), width (w) and height (h) of $15.38 \times 11.12 \times 4.30$ nm^3, respectively. The pulling layer thicknesses (pt) was considered to be three atomic layers wide. For the subsequent MD simulations, the molecular dynamics program GROMACS 5.0.4 package [33] was used. For aragonite interactions, newly-developed $CaCO_3$ forcefield [36], that describes angle, planar, dihedral, electrostatic and van der Waals interactions, was implemented.
The model in question was minimized and equilibrated in the NPT (isothermal-isobaric) ensemble for 10 ns at 300 K and 1.013 bar. The tablet did not show any significant changes neither in structural ordering nor in cell dimensions. The last frames were used to create notched systems as follows: The simulation boxes were extended 12 nm along l and h, leaving as much empty space as required to allow the tablet extension during pulling simulations. The periodic vector through the width w was not extended, resulting in tablets of infinite length along w-direction. Then, the v-shaped notches were introduced by removing atoms. The cut lines followed the (101) and ($\bar{1}$01) lattice planes, which resulted in an opening angle of 84.4 °. Such cut lines impose the removal of one calcium atom per carbonate group, preserving the electroneutrality of the systems.
Whereas in the MD calculations, the simulation box, in which the aragonite tablets were pulled, was repeated periodically in all three dimensions using 2 fs time steps. Van der Waals interactions were calculated using a cutoff of 1.0 nm. The Particle

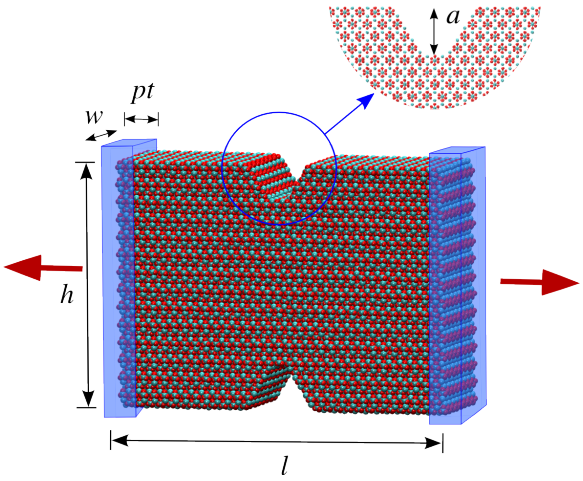

Figure 2: Double-notched all-atom model of an aragonite tablet. Oxygen and carbon atoms of carbonate groups are shown in cyan and red beads, respectively. Calcium atoms are shown with green beads. The dimension a (center) denotes the notch depth, while h, l, w and pt represent the height, length, width and pulling layer thickness, respectively. Pulling directions are perpendicular to the notch depth, which is marked by red arrows. Inset: enlargement of the front view of v-notch region.

Mesh Ewald (PME) method [6] was chosen to account for long-range electrostatic interactions. To increase the simulation time step, a linear constraint solver for molecular simulations (LINCS) [12] was used to constrain all bond vibrations. The Nosé-Hoover [24, 13] temperature coupling was applied with a coupling time constant of 0.1 ps.

Fig. 2 shows an aragonite notched model with loading conditions and representative dimensions. The aragonite tablet model was not constrained at any point (which allows for rigid body motions) to capture a natural behavior in the simulations. The system was further equilibrated in the NVT (canonical ensemble, amount of substance N, volume V and temperature T are conserved) for 10 ns at 300 K. To avoid tablet drifting, two cuboid volumes parallel to the (100) lattice plane were restrained, each cuboid volume containing the three outermost layers of $CaCO_3$ atoms. This resulted in a system of 66,720 atoms.

Once the equilibration of the system was achieved, a force-probe Molecular Dynamics (FPMD) simulation [10] was employed to enforce an external load. The restrained layers were released and pulled axially outwards with a spring-like force applied to the outer surfaces, with a constant velocity of 10 nm ns^{-1} and a spring constant of 1000 kJ mol^{-1} nm^{-2}. FPMD simulations were performed until tablet rupture, which usually occurred within 13 ns. Altogether, five FPMD simulations were performed. The obtained results were later post-processed to obtain critical material parameters, as well as the phase-field transition width and crack resistance energy.

Postulated in 1920, though still in force, the Griffith's energy-based analysis of cracks [9] states that the fracture strength is always lower than theoretical cohesive strength and attributes this discrepancy to the inherent defects in brittle materials,

leading to stress concentration.
One of the underlying principles of fracture mechanics is that crack propagation occurs when the released elastic strain energy is at least equal to the energy required to generate new crack surface. The Griffith's energy criterion for fracture of brittle materials can then be written as

$$\sigma_f = \frac{1}{\alpha}\left[\frac{2E\gamma}{\pi a}\right]^{1/2} \quad , \tag{1}$$

where σ_f is the rupture strength, a is the notch depth, γ is the surface energy, E is the Young's modulus, and α is a geometry correction factor. For double edge notched tension of a semi-infinite tablet with notch depth a and tablet height h, α reads [29]

$$\alpha = 1.12 + 0.43\left[\frac{a}{h}\right] - 4.79\left[\frac{a}{h}\right]^2 + 15.46\left[\frac{a}{h}\right]^3 . \tag{2}$$

It is now assumed that the available external and internal energy is transferred into surface energy. In what brittle fracture regards, dissipation and kinetic energy are neglected. This results in the so-called Griffith energy balance where the energy release rate G is equal to 2γ in $\mathrm{J/m^2}$. The mechanical energy release rate in the $CaCO_3$ geometry is the amount of energy per unit area that is supplied by the elastic energy stored in the system.
The energy release rate can alternatively be calculated by integrating the stress-strain curve with respect to strain [20, 17]

$$G = l\int_0^{\varepsilon} \sigma(\varepsilon')d\varepsilon', \tag{3}$$

where l is the model width in the loading direction, see Fig. 2, and σ is the loading direction component of the stress well ahead of the crack tip. At a strain above ε_c, crack propagation at constant velocity is achieved after an initial transient [20].

2.2 Brittle Fracture Modeling using the PFM Approach

The macroscopic modeling of brittle fracture is based on the PFM approach, which has been widely discussed in several research works, see, e.g. [3, 22, 35] for an overview. In this, a phenomenological phase-field variable ϕ is introduced, which approximates the sharp interface of the crack by a diffusive transition zone. Thus, the global potential energy function $\mathcal{F}$ can be written with the help of ϕ and its gradient as an integral over the whole body ([4, 8, 19, 21]) as

$$\mathcal{F}(\phi, \operatorname{grad}\phi, \boldsymbol{\varepsilon}) = \int_V \left[\Psi_{elast}(\phi, \boldsymbol{\varepsilon}) + \Psi_{crack}(\phi, \operatorname{grad}\phi)\right] \mathrm{d}v \tag{4}$$

with $\boldsymbol{\varepsilon}$ being the linear strain tensor. The phase-field variable $\phi \in [0, 1]$, in the sense of an indicator function, represents the crack state, where $\phi = 0$ for a cracked state

and $\phi = 1$ for an undamaged state. The fracture energy Ψ_{crack} is defined as

$$\Psi_{crack}\,(\phi, \operatorname{grad}\phi) = \frac{G}{4\epsilon}(1-\phi)^2 + G\,\epsilon\,|\operatorname{grad}\phi|^2, \tag{5}$$

where ϵ is an internal length related to the width of the diffusive crack transition zone. As the degradation of the material is assumed to occur only under tension or shear, one applies an additive splitting of the linear elastic energy into a positive part Ψ^+_{elast}, that considers the tension and shear responses, and a negative part Ψ^-_{elast}, that considers the compression response. Moreover, the degradation function $g(\phi)$ can simply be defined in a quadratic form as $g(\phi) = [(1-\eta)(\phi)^2 + \eta]$ to obtain

$$\Psi_{elast}\,(\phi, \boldsymbol{\varepsilon}) = g(\phi)\;\Psi^+_{elast} + \Psi^-_{elast}\,. \tag{6}$$

Here, η is a residual stiffness added for numerical stability purpose. The linear elastic stress $\boldsymbol{\sigma}$ is obtained through the derivation of the phase-field potential with respect to the strain tensor, see [23].

$$\boldsymbol{\sigma}(\phi, \boldsymbol{\varepsilon}) = \frac{\partial \mathcal{F}}{\partial \boldsymbol{\varepsilon}} = g(\phi)\;\frac{\partial \Psi^+_{elast}}{\partial \boldsymbol{\varepsilon}} + \frac{\partial \Psi^-_{elast}}{\partial \boldsymbol{\varepsilon}}\,. \tag{7}$$

Furthermore, the momentum balance equation under the assumptions of a quasi-static state and neglecting the body forces can be expressed as

$$\operatorname{div}\boldsymbol{\sigma} = \mathbf{0}\,, \tag{8}$$

allowing the computation of displacement field $\mathbf{u}$. To this end, the evolution of the phase field is derived using the Allen-Cahn model,which describes the process of crack evolution via a reaction-diffusion equation as

$$\begin{aligned} \dot{\phi} &= \frac{\partial \phi}{\partial t} = -M\frac{\partial \mathcal{F}}{\delta \phi} \\ &= -M\left[2\,(1-\eta)\phi\;\Psi^+_{elast} - \frac{G}{2\epsilon}(1-\phi) - 2\,G\,\epsilon\operatorname{div}\operatorname{grad}\phi\right], \end{aligned} \tag{9}$$

where $M \geq 0$ represents a mobility constant.
For the numerical implementation of the PFM problem, an initial boundary-value problem of mode-I fracture, illustrated in Figure 3, is solved using the finite element package FlexPDE.
The numerical solution is computed considering quadratic shape functions for the displacement and the phase-field variable, and the time integration is applied using the 2$^{\text{nd}}$-order backward difference formula (BDF2), where a time-step automatic adaptivity is also employed. Moreover, a fixed mesh, refined in the area between the notches, is implemented. A plane stress, linear elastic model is used to reproduce the MD simulation. Under this setup, the stress is applied until instantaneous rupture of the plate takes place.
The material parameters, E, ϵ and G, for the PFM of the aragonite plate were directly derived from the outcomes of the MD simulations as will be discussed in the next section. Therewith, the obtained values were $E = 126$ GPa for the Young's modulus. The crack resistance (or energy release rate) was found to be $G = 2.091$

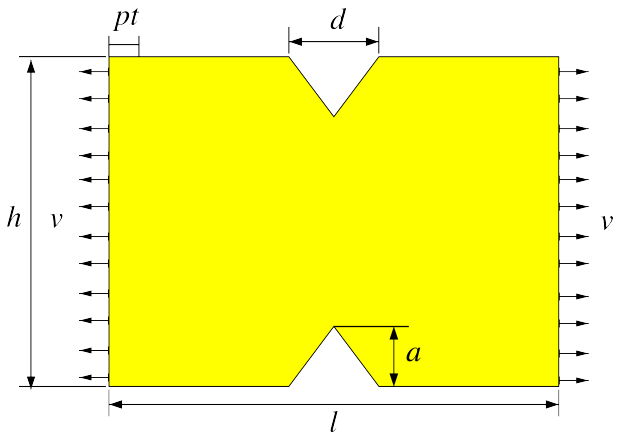

Figure 3: Boundary conditions of the IBVP (load-controlled). For the boundary layers with width pt, $\nu = 0$ and zero-stress in vertical direction. In the middle of the extreme edges (left and right), two points are fixed in the vertical direction to prevent a rigid body motion. The dimensions here are h=11.2 nm, l=15.3 nm, d=3.08 nm, and a=1.84 nm.

J/m^2 and the internal length scale $\epsilon = 0.05$ nm. The values of the mobility and the residual stiffness parameters were set to $M = 10 \times 10^9$nm^2/Ns and $\eta = 10^{-5}$, respectively, whereas the applied Poisson's ratio is $\nu = 0.44$. The material properties such as Possion's ratio ν and the density ρ were benchmarked with the aragonite-related literature ([1, 2, 7, 25]), whereas the mobility parameter M and the residual stiffness parameter η are in good agreement with the ranges proposed in, e.g., [18, 23].

2.3 Results and Discussion

As stated previously, to examine the fracture behavior at atomistic scale of aragonite, monotonic tension tests were performed by means of FPMD. The molecular system was loaded by moving virtual springs applied to the outer surfaces of the tablets with constant velocity. The force is obtained directly from the resultant spring force at the boundaries. Accordingly, the stress is computed by dividing the spring force by the cross sectional area comprehended between two notches. Moreover, the relative displacement of atoms was measured between the center of mass of both pulling layers. Here, the engineering strain is obtained by dividing the total displacement of the center of mass of any pulling layer by the original distance between this layer and the center of specimen. The crystals deformed during the FPMD simulations until the externally applied stress reached the ultimate tensile strength σ_f, resulting in a sudden rupture. Due to the chemical structure of calcium carbonate $[Ca^{2+}][CO_3^{2-}]$, and its arrangement in compact crystal, it is not always possible to have symmetric notches on both edges as well as notches at the exact center of all tablets of $CaCO_3$ models. Therefore, the v-notches in the tablets are not sharp, and the notch tips can have, either, single or double $CaCO_3$ units (enlarged view in Fig. 2). Thus, different crack propagations were observed in the tablet models, e. g., the crack starts at the

top edge, bottom edge or at both edges simultaneously (shown in Fig. 4). For all simulations, the cracks propagated with an s-shape along the (101) and ($\bar{1}$01) lattice planes, as expected.

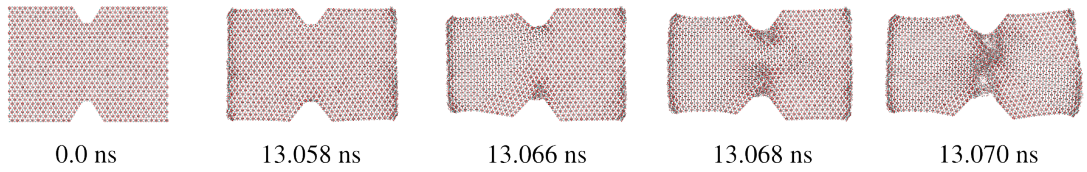

Figure 4: Rupture of the double-notched aragonite tablets. The snapshots show the fracture of the aragonite tablets under constant pulling velocity. As the two atom groups at the ends are pulled, the tablets slightly stretch and break abruptly around the notch. Here, the crack initiates at the bottom, though, is propagated from both sides and with an s-shape.

Fig. 4 shows snapshots of the rupture processes observed in the $CaCO_3$ tablet models. The model was loaded with a constant velocity for 12.88 to 13.056 ns, without observing crack initiation. However, the crack initiation took place during the following 0.012 ns, inducing an instantaneous total failure.
The results describe a good agreement with the expectations. First of, the energy release rate G can be calculated using the MD results together with either Griffith's criterion given in Eq. (1) or by use of Eq. (3). Both equations confirm that the fracture of the $CaCO_3$ tablet occurs at a value $G \approx 2.091\,\mathrm{J/m^2}$. This value is slightly lower than the theoretical values of G for $CaCO_3$ ($2.10-3.74\,\mathrm{J/m^2}$), which can be found in the literature [1, 2, 7], though this difference is merely negligible. Therefore, $G = 2.091\,\mathrm{J/m^2}$ is adopted for the PFM.
To avoid model dependency in MD simulations, five different aragonite tablet models were considered, and the stress-strain curves were jointly analyzed. The recovered elasticity modulus E of aragonite ranges between 106 to 148 GPa, which is in the range of experimental and theoretical studies, see [1, 2, 7]. With regard to the ultimate tensile strength, the resulting MD simulations value of the aragonite notched samples is 4.6 GPa. This value is slightly lower than the theoretical strength of flawless minerals, which was estimated to lie in the range of 5 to 10 GPa [32].
Fig. 5 shows the force-displacement curves of the continuous PFM (considering a Young's modulus of $E = 126$ GPa) and all-atom simulations. With regard to the force at failure, the resulting MD simulations value of the aragonite notched samples is 47 μN and the nonlinear behavior, which is due to the potential energy nonlinearities, is clearly observed. Although, a linear elastic model was considered for the PFM, an outstanding correlation of the results is observed.
Phenomenologically, the s-shaped crack propagation (along the (101) and ($\bar{1}$01) lattice planes) is obtained in both MD and PFM approaches. Moreover, the ultimate tensile strength obtained in the PFM simulations falls perfectly into the ranges described in the all-atom simulations. Nevertheless, a discrepancy between the two schemes can be seen which can be traced to two main reasons: On the one side, the boundary conditions in the MD simulation allow for rigid body rotations and translations, which are constrained in the continuum model by fixing the vertical displacement of two points. This fixation causes an artificial symmetry and si-

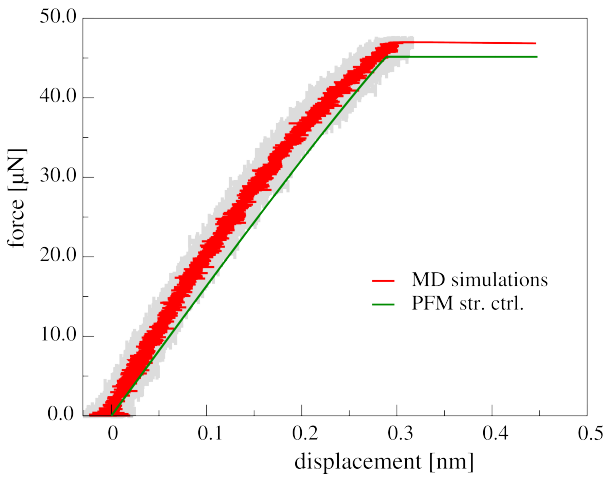

Figure 5: Force-displacement curves for the aragonite tablet models. The red line is the averaged force-displacement curve from the MD simulations, and the gray shaded area indicates the standard error deviation. The green line indicate the force-displacement curves obtained from the PFM stress-controlled simulation.

multaneously stiffens the material. On the other side, the PFM considers a linear elastic material response, which is not able to account for the inherent material non-linearities. As seen in Fig. 5, these non-linearities are naturally captured in the atomistic simulations.
An important outcome, particularly for the phase-field parameters, is the theoretical and numerical consistency of the critical energy release rate G, and a potential relationship between the molecular transition (distortion) zone and the phase-field transition width governed by the internal length parameter ϵ. The former can be estimated by means of the Griffith's theory or by integration of the stress-strain curve, yielding a value within the literature range (approximately 2.1 J/m^2). The latter can be obtained by measuring the cracked surfaces in a straightforward post-processing step. The results of the MD and PFM simulations are shown in Fig. 6. Taking into account the density plot of the MD and overlapping it with the resultant intact-to-cracked material transition of the PFM, as seen in Fig. 6, the phenomenological correlation is evident.

3 Conclusions

As shown in this work, the efficiency of continuum mechanics allows to infer mechanical properties from the molecular scale, which is the key to understand a material's interplay of the atomic structure and its overall performance. Through an atomistic obtention of the material parameters, the PFM presented in this work observes a fair convergence, and more important remains qualitatively and quantitatively within the outcomes of MD simulations and the benchmarked literature. Moreover, a correlation between the phase-field parameter ϵ (which is of extreme importance for convergence) and an MD transition zone was captured for the first time. Through further study, this could result in a physical meaning and obtention of the parameter value, which is up to date fitted according to each model. Moreover, the observed

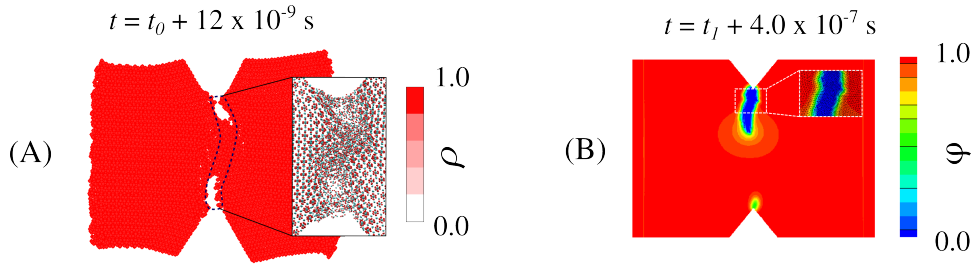

Figure 6: Crack initiation and propagation comparison: (A) Density plots of atoms in MD simulations (ρ stands for density). The s-shaped crack is illustrated with a dotted line, and the inset shows an all-atom simulation snapshot of the crack propagated area. (B) PFM results for stress-controlled simulations (ϕ stands for the damage phase-field, blue corresponds to cracked material, and red refers to undamaged material). The times t0 and t1 are the total loading times before crack initiation in MD (t_0 = 13056 ps) and PFM stress-controlled (t_1 = 0.0403089 s) respectively.

molecular dissipative zone between the undamaged and cracked material allows to think that in fact, brittle fracture observe a transition zone, under a purely atomistic standpoint.

The presented bottom-up approach thus represents, an important tool in the field of artificial material design. The approach proposed here can be extended to other bio-materials, and partially or highly ordered polymeric and composite materials, which are characterized by a similar interplay of structure and mechanics on different scales.

References

[1] F. Barthelat and H. D. Espinoza. Elastic properties of nacre aragonite tablets. In SEM Annual Conference and Exposition on Experimental and Applied Mechanics, page 187, 2003.

[2] F. Barthelat, C. M. Li, C. Comi, and H. D. Espinosa. Mechanical properties of nacre constituents and their impact on mechanical performance. J. Mater. Res., 21:1977–1986, 2006.

[3] M. J. Borden, C. V. Verhoosel, M. A. Scott, T. J. R. Hughes, and C. M. Landis. A phase-field description of dynamic brittle fracture. Comput. Method. Appl. M., 217–220:77–95, 2012.

[4] B. Bourdin, G.A. Francfort, and J.J. Marigo. The variational approach to fracture. J. Elasticity, 91:5–148, 2008.

[5] Murat Cetinkaya, Senbo Xiao, Bernd Markert, Wolfram Stacklies, and Frauke Gräter. Silk fiber mechanics from multiscale force distribution analysis. Biophys J, 100(5):1298–1305, Mar 2011.

[6] T. Darden, D. York, and L. Pedersen. Particle mesh ewald: An n log (n) method for ewald sums in large systems. J. Chem. Phys., 98:10089–10092, 1993.

[7] T. Z. Forbes, A. V. Radha, and A. Navrotsky. The energetics of nanophase calcite. GeoChim. Cosmochim. Ac., 75:7893–7905, 2011.

[8] G.A. Francfort and J.-J. Marigo. Revisiting brittle fracture as an energy minimization problem. J. Mechan. and Phys. Solids., 46:1319–1342, 1998.

[9] A. A. Griffith. The phenomena of rupture and flow in solids. Phil. Trans. Roy. Soc. Lond. A, 221:163–198, 1921.

[10] H. Grubmüller, B. Heymann, and P. Tavan. Ligand binding: molecular mechanics calculation of the streptavidin-biotin rupture force. Science, 271(5251):997–999, Feb 1996.

[11] C. A. Hernandez Padilla and B. Markert. A coupled ductile fracture phase-field model for crystal plasticity. Continuum Mech. Thermodyn. DOI:10.1007/s00161-015-0471-0, pages 1–10, 2015.

[12] B. Hess, H. Bekker, H. J. C. Berendsen, and J. G. E. M. Fraaije. Lincs: a linear constraint solver for molecular simulations. J. Comput. Chem., 18(12):1463–1472, 1997.

[13] W. G. Hoover. Canonical dynamics: Equilibrium phase-space distributions. Phys. Rev. A, 31(3):1695–1697, 1985.

[14] W. Humphrey, A. Dalke, and K. Schulten. Vmd: visual molecular dynamics. J. Mol. Graph., 14(1):33–38, 1996.

[15] G. R. Irwin. Analysis of stresses and strains near the end of a crack traversing a plate. J Appl Mech, 24:361–364, 1957.

[16] R. K. Kalia, A. Nakano, A. Omeltchenko, K. Tsuruta, and P. Vashishta. Role of ultrafine microstructures in dynamic fracture in nanophase silicon nitride. Phys. Rev. Lett., 78:2144, 1997.

[17] H. Kikuchi, R. K. Kalia, A. Nakano, P. Vashishta, P. S. Branicio, and F. Shimojo. Brittle dynamic fracture of crystalline cubic silicon carbide (3c-sic) via molecular dynamics simulation. J. Appl. Phys, 98:103524, 2005.

[18] C. Kuhn and R. Müller. A continuum phase field model for fracture. Eng. Fract. Mech., 77:3625 –3634, 2010.

[19] C. Kuhn, A. Schlüter, and R. Müller. A phase field approach for dynamic fracture. PAMM, 13(1):87–88, 2013.

[20] B. Lawn. Fracture of Brittle Solids. Cambridge University Press, Cambridge, 1993.

[21] B. Markert and Y. Heider. Coupled multi-field continuum methods for porous media fracture. In Miriam Mehl, Manfred Bischoff, and Michael Schäfer, editors, Recent Trends in Computational Engineering - CE2014, volume 105 of Lecture Notes in Computational Science and Engineering, pages 167–180. Springer International Publishing, 2015.

[22] C. Miehe, M. Hofacker, and F. Welschinger. A phase field model for rate-independent crack propagation: Robust algorithmic implementation based on operator splits. Comput. Method. Appl. M., 199:2765 –2778, 2010.

[23] C. Miehe, F. Welschinger, and M. Hofacker. Thermodynamically consistent phase-field models of fracture: Variational principles and multi-field fe implementations. Int. J. Numer. Meth. Eng., 83:1273–1311, 2010.

[24] S. Nosé. A molecular dynamics method for simulations in the canonical ensemble. Mol. Phys., 52(2):255–268, 1984.

[25] S. P. Patil, Y. Heider, C.A. Hernandez-Padilla, E.R. Cruz-Chú, and B. Markert. A combined molecular dynamics-phase-field modeling approach to fracture. Comput. Methods Appl. Mech. Engrg., DOI: 10.1016/j.cma.2016.04.005вГК, 2016.

[26] S. P. Patil, B. Markert, and F. Gräter. Refining a bottom-up computational approach for spider silk fibre mechanics. Proceedings of the 3rd GAMM Seminar on Continuums Biomechanics, II-21:75–87, 2012.

[27] Sandeep P. Patil, Bernd Markert, and Frauke Gräter. Rate-dependent behavior of the amorphous phase of spider dragline silk. Biophys J, 106(11):2511–2518, Jun 2014.

[28] Sandeep P. Patil, Senbo Xiao, Konstantinos Gkagkas, Bernd Markert, and Frauke Gräter. Viscous friction between crystalline and amorphous phase of dragline silk. PLoS One, 9(8):DOI: 10.1371/journal.pone.0104832, 2014.

[29] N. Perez. Fracture Mechanics. Kluwer Academic Publisher Group, 2004.

[30] C. L. Rountree, R. K. Kalia, E. Lidorikis, A. Nakano, L. van Brutzel, and P. Vashishta. Atomistic aspects of crack propagation in brittle materials: Multimillion atom molecular dynamics simulations. Annu. Rev. Matter. Res., 32:377–400, 2002.

[31] C. L. Rountree, S. Prades, D. Bonamy, E. Bouchaud, R. Kalia, and C. Guillot. A unified study of crack propagation in amorphous silica: Using experiments and simulations. J. Alloy. Comp., 434–435:60–63, 2007.

[32] C. H. Scholz. The Mechanics of Earthquakes and Faulting. Cambridge University Press, 2^{nd} edition, 2002.

[33] D. van der Spoel, E. Lindahl, B. Hess, G. Groenhof, A. E. Mark, and H. J. Berendsen. Gromacs: fast, flexible, and free. J. Comput. Chem., 26(16):1701–1718, 2005.

[34] P. Vashishta, M. E. Bachlechner, T. Campbell, R. K. Kalia, H. Kikuchi, S. Kodiyalam, A. Nakano, S. Ogata, F. Shimojo, and P. Walsh. Multimillion atom simulation of nanostructured materials on parallel computers. Prog. Theor. Phys. Supplement, 138:135–170, 2000.

[35] J. Vignollet, S. May, R. de Borst, and C. V. Verhoosel. Phase-field models for brittle and cohesive fracture. Meccanica, 49:2587–2601, 2014.

[36] S. Xiao, S. A. Edwards, and F. Gräter. A new transferable forcefield for simulating the mechanics of $caco_3$ crystals. J. Phys. Chem. C, 115:20067–20075, 2011.

[37] S. P. Patil. Doctoral dissertation: Multiscale modeling of spider dragline silk. RWTH Aachen University, 2015.

Bernd Markert, Institute of General Mechanics, RWTH Aachen University, Templergraben 64, 52062 Aachen, Germany
Sandeep P. Patil, Institute of General Mechanics, RWTH Aachen University, Templergraben 64, 52062 Aachen, Germany